




On 3D printing of low-cost sensors using recycled PET

RUPINDER SINGH^{1,*}, BHANU PRATAP SINGH², AMRINDER PAL SINGH²,
VINAY KUMAR^{3,4}, RANVIJAY KUMAR⁴, MAHDI BODAGHI⁵, AHMAD SERJOUEI⁵
and YANG WEI⁵

¹Department of Mechanical Engineering, National Institute of Technical Teachers Training and Research, Chandigarh, India

²Department of Mechanical Engineering, Panjab University, Chandigarh, India

³Department of Mechanical and Production Engineering, Guru Nanak Dev Engineering College, Ludhiana, India

⁴Department of Mechanical Engineering, University Center for Research and Development, Chandigarh University, Mohali, India

⁵Department of Engineering, Nottingham Trent University, Nottingham, UK
e-mail: rupindersingh@nitttrchd.ac.in

MS received 16 May 2022; revised 15 September 2022; accepted 28 October 2022

Abstract. Polyethylene terephthalate (PET) thermoplastic polyester is durable, formable material that is widely used to manufacture consumer products like sailcloth, sailing spinnakers, food-grade containers, etc. for commercial and engineering applications. The recycling of PET is still a challenge because of its abundance, especially in low-income/developing countries. The present study reports the recycling of PET by utilizing the primary (1°) recycled PET (R-PET) for 3D printing-based sensor applications with the idea of converting waste to wealth. The investigations were performed on PET-based waste collected from institute campus canteens (in form of used food containers/soft drink bottles) after ascertaining their rheological, mechanical, morphological, bonding, and sensing capabilities. The sensing capabilities of R-PET were explored by performing a ring resonator test of a 3D-printed substrate using a vector network analyzer (VNA). The result of the study outlined that R-PET-based sensors may be used in sailcloth, and sailing spinnakers to monitor the location of boats in a shipyard/dock.

Keywords. Polyethylene terephthalate; recycling; screw extrusion; 3D printing; sensor applications.

1. Introduction

The industrial applications of PET thermoplastic for manufacturing consumer products like bottles, cans, storage tanks, etc. have been widely reported [1]. The finite element, thermal and mechanical analysis performed on PET to fabricate thin and durable products like tubes, bottles (even with complex geometry, colors), and sheets have been outlined by some researchers to reduce the cost of manufacturing and producing attractive household goods [1, 2]. Over the past decade, researchers are exploring the non-conventional engineering applications of PET and glycol-added PET (known as PETG) for construction and non-structural activities by 3D and 4D printing processes to address the environmental issues raised by excessive use of PET and PETG around the globe [3, 4]. The reports of manufacturing one million plastic bottles in a minute have highlighted the alarming environmental issues for mankind

[5] that may be resolved effectively by melt processing-based recycling of plastic solid waste through additive manufacturing (AM) [6, 7]. In some recent studies, PET chip-based sensors for the detection of food poisoning bacteria (salmonella), luminescence detection, and magnetic devices also have been reported. The screen-printed and laser-cut PET chip incorporated in a self-driven type electrochemical sensor is capable to detect salmonella bacteria within 20 min without induction of external load on the pressure chamber where the test sample is located. Similarly, a PET-polyvinyl alcohol (PVA) based flexible composite sensor may be used to enhance the magneto-caloric effect of magnetic devices [8–10]. The investigations performed on mechanical properties of composites and advanced materials like PETG to prepare fused deposition modeling (FDM) based meta-materials have outlined the sustainability of AM processes to use recycled plastic for the fabrication of novel consumer products [11, 12]. Thermoplastic composites are prepared by reinforcement of carbon fibers in high-density polyethylene (HDPE), PETG,

*For correspondence

and polypropylene (PP) for sensor and antenna applications and the use of PET for high-frequency signals transmission has been reported recently [13, 14]. Some advanced engineering applications of thermoplastic composites (reinforced with graphene, Ni, polypyrrole, glass fibers, etc.) like polyethylene naphthalene (PEN), polyvinylidene fluoride (PVDF), PET, PETG in electromagnetic interference shielding, non-structural engineering, 4D printing, and wearable textile antennas highlighted the novel use of recycled polymers for non-traditional areas of medical and engineering sciences [15–18].

The use of PETG for manufacturing packaging material and sailcloth has been observed as a harmful practice for environmental health and marine life due to challenges in the management of waste PETG. PET has been reported as an alternative to PETG based on life cycle analysis for sailcloth, bottling, packaging, and sailing spinnaker manufacturing because of its durability and high chemical stability [19, 20]. The past three decades have witnessed an exponential increase in the use of PET. A few studies on polymer degradation and stability (e.g. the use of poly-ionic liquid catalysts) have been witnessed to reuse and recycle PET for waste management [21]. Recycling of solid plastic waste (SPW) both thermoplastics (like HDPE, acrylonitrile butadiene styrene (ABS)) and thermosetting (like melamine-formaldehyde, bakelite, etc.) has been observed as a novel route to reuse the plastics for AM based 3D/4D applications [22–24]. Even the composite prepared from recycled PVDF and PET has useful applications in the construction and maintenance of built structures due to acceptable mechanical and bonding strength when used with the base material of structures [25, 26]. Beyond the construction and non-structural engineering applications, recycling of low-density polyethylene (LDPE), LDPE-bakelite composite, and ABS also have been reported in the literature for sensor and antenna fabrication by utilizing FDM-based 3D printing process [27, 28].

The literature review highlighted that PET is a highly used thermoplastic for various commercial and engineering practices. But hitherto little has been reported on the in-house processing route to recycle PET for 3D printing-based sensor fabrication and managing the waste PET in academic institutes. The low-cost R-PET sensor embedded in the sailcloth/sailing spinnaker may be used by fishermen in low-income/developing countries living in coastal areas to monitor the boats parked in the shipyards. The present study is performed for the 3D printability of R-PET sensors after ascertaining the rheological, mechanical, morphological, bonding, and sensor properties of waste PET plastic. The experimentation was performed on R-PET shredded for melt flow index (MFI) testing for successful screw extrusion and 3D printing. Mechanical properties were ascertained and optimized for acceptable durability. Further, sensor properties were investigated by performing a ring resonator test of a 3D-printed R-PET substrate using a vector network analyzer (VNA).

2. Experimentation

2.1 PET shredding, rheological analysis and screw extrusion

The SPW of used PET bottles collected from the institute campus were shredded in a Felfil shredder unit (Make: Felfil, Italy) equipped with counter blades to obtain a uniform size of PET grains. After ascertaining the rheological property of R-PET based on MFI (as per ASTM D1238), the R-PET granules were screw extruded (using a Felfil Evo extruder, Italy). Taguchi L_8 array was used to design the experiment for filament extrusion. The mechanical properties acceptable for filament extrusion and 3D printing were ascertained and optimized.

2.2 Electrical, bonding and sensor characterization

After ascertaining the suitable extrusion parameters (based on mechanical analysis and parametric optimization) for 3D printing of R-PET, the electrical (voltage-current (V-I)) properties of the filament were ascertained by the source meter unit (Make: Keithley, USA). The bond and crystal structure of the filament were investigated by Fourier-transformed infrared (FTIR) and X-ray diffraction (XRD) analysis. 3D printing of R-PET was performed on an open-source FDM unit (Make: Creality Ender-3, India) to fabricate the substrate of a ring resonator. The ring resonator was tested on VNA and the output was used to perform the simulation of an R-PET-based antenna using high-frequency structure simulation (HFSS) software for sensor/monitoring applications. Figure 1 shows the methodology for the experimentation.

3. Results and discussion

3.1 Rheological analysis

The shredded PET granules were prepared at 30 rpm shredding speed and 25 Nm torque to obtain a uniform size of feedstock (figure 2). The MFI of regular-size granules was investigated at different temperatures i.e., 230°C,

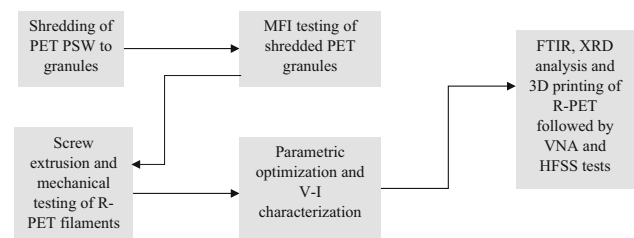


Figure 1. Work methodology for the present work.

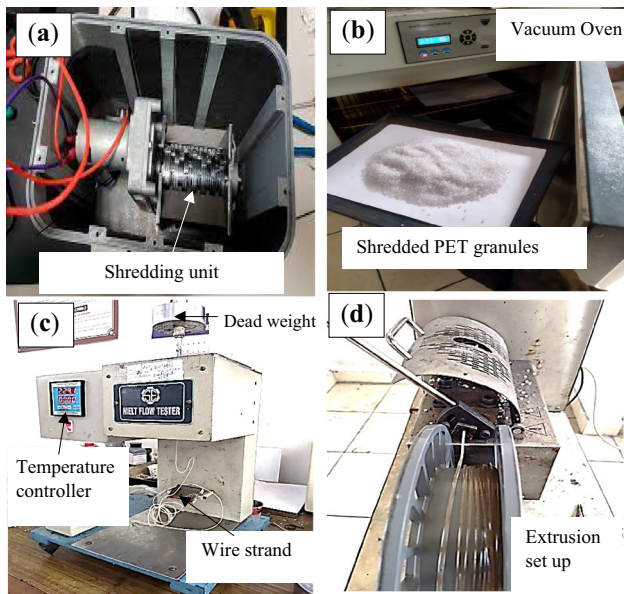


Figure 2. Shredding unit (a), Pre-heating of shredded PET granules (b), MFI testing set up (c) and Extrusion set up (d).

240°C, etc. to ascertain the acceptable conditions (temperature, applied load) for rheological analysis (MFI, density, viscosity, etc.) of R-PET. The results obtained for MFI are shown in table 1.

As observed in table 1, the MFI of R-PET increased significantly from 3.59 to 22g/(10 min) with an increase in temperature from 230°C to 250°C without any pre-heating, but in visual observation, the surface of wires prepared was observed to rough with the increase in MFI. As a thumb rule, higher MFI helps to prepare the thin section, but for commercial applications in 3D printing, MFI in the range of 2.5-4.0g/10 min is preferred as one does not require any change in hardware/software settings of commercial printers to 3D print functional prototypes. Also, during a pilot study, R-PET grains pre-heated at 60°C (20°C below glass transition temperature (T_{GT})) before MFI at 240°C showed a smooth surface along the cross-section of wire samples (visual observation) may be due to the removal of moisture during the pre-heating process. At 250°C MFI was

Table 1. MFI results for PET.

Die Temperature (°C)	MFI g/(10min)
230 (without pre-heating)	3.59 ± 0.12
240 (without pre-heating)	6.13 ± 0.20
250 (without pre-heating)	22.01 ± 0.31
240 (Pre-heated PET at 60°C)	5.65 ± 0.19

The applied load for the MFI test of R-PET was kept fixed i.e., 3.8 kg in all cases (as per ASTM D1238)

significantly increased but poor surface characteristics in terms of surface finish were observed. Based on MFI observations (table 1), 240°C and 250°C were not considered appropriate temperatures for the processing of R-PET. MFI at 3.59g/(10 min) at 230°C was considered the acceptable condition to study the rheological and mechanical properties of R-PET for 3D printing.

3.2 Mechanical analysis

Based on MFI results, 230°C screw extrusion temperature for R-PET was considered to prepare filament. Since heat treatment also indicated an effect on surface properties, it was also taken into the account to prepare the design of the experiment (DoE) for filament fabrication. Taguchi L_8 orthogonal array (mixed level design) was used to prepare DoE in which 04 levels of processing temperature (210, 215, 220, 225°C), 02 levels of processing conditions (non-heat treated (NHT) and heat-treated (HT) at 60°C), and 02-speed levels (3 and 5 rpm) were considered for Felfil Evo filament extruder to obtain R-PET filament samples. The same was selected based on pilot runs and available equipment.

The 08 sets of filament samples (of diameter (ϕ) 1.75 ± 0.05 mm and cross-section area 2.4 ± 0.1 mm²) with three repetitions were fabricated by screw extrusion process as per DoE. The mechanical properties of the filaments were tested by a universal testing machine (UTM). The V-I characteristics of fabricated filament samples were also investigated for a fixed potential difference of 1Volt (V) (for low potential field applications (like sailcloth, sailing spinnakers, food-grade containers, etc.), which may be provided by small button cells as an energy storage device (ESD)). It may be noted that the flow of current and resistance offered may be checked at a higher voltage level, but this will lead to the requirement of high capacity of ESD, which may be undesirable in field applications mainly because of space constraints. The results obtained for the mechanical and electrical properties (average of three observations) of R-PET filaments are shown in table 2.

3.2.1 Parametric optimization for E: The analysis of variance (ANOVA) for E (as per table 2) was performed based on the signal-to-noise (SN) ratio (table 3) for the larger the better type case. One of the reasons for selecting E for ANOVA was to ensure better sensing/detection capability. It may be noted that E is the slope of the stress-strain curve in the range of linear proportionality of stress to strain. The greater the E, the stiffer the material. In other words, the elastic strain resulting from the application of given stress is smaller. This will help to control the variation in dielectric constant (ϵ_r) and loss tangent ($\tan\delta$). Hence variation in resonance frequency will be less if E is more. So, better sensing/detection capabilities may be

Table 2. Mechanical and electrical properties of R-PET filament samples.

Sample	Processing temperature (°C)	Processing condition	Speed (rpm)	Peak			Break Elongation (mm)	Strength at Peak (MPa)	Strength at Break (MPa)	Young's Modulus (E) (MPa)	Modulus of toughness (MOT) (MPa)	Current (A)	Resistance (Ω)
				Peak Load (N)	Elongation (mm)	Load (N)							
S1	210	NHT	3	81.3 ± 0.9	2.1 ± 0.2	73.2 ± 0.8	3.36 ± 0.2	33.82 ± 1.8	32.44 ± 1.9	644.1 ± 4.1	1.27 ± 0.1	0.013 ± 0.001	79.38 ± 1.1
S2	210	HT	5	105.3 ± 1.8	2.94 ± 0.2	104.9 ± 1.6	5.25 ± 0.2	32.93 ± 1.8	31.03 ± 1.8	637.8 ± 3.5	1.07 ± 0.2	0.014 ± 0.001	69.23 ± 1.0
S3	215	NHT	3	108 ± 1.6	2.94 ± 0.1	97.0 ± 1.5	6.51 ± 1.5	44.84 ± 2.0	40.36 ± 2.1	610.0 ± 2.9	2.28 ± 0.8	0.016 ± 0.001	60.00 ± 0.9
S4	215	HT	5	78.9 ± 1.0	2.31 ± 0.3	71.0 ± 0.9	3.78 ± 0.3	32.82 ± 1.0	29.54 ± 1.1	568.3 ± 2.3	1.39 ± 0.3	0.012 ± 0.002	82.78 ± 1.2
S5	220	NHT	5	125 ± 2.3	3.36 ± 0.4	112 ± 2.1	4.41 ± 0.3	51.79 ± 1.7	46.61 ± 1.8	616.5 ± 2.4	2.36 ± 0.8	0.012 ± 0.001	83.43 ± 1.1
S6	220	HT	3	99 ± 1.4	3.57 ± 0.4	89.1 ± 1.3	5.25 ± 0.4	41.18 ± 1.7	37.06 ± 1.7	461.4 ± 1.9	2.43 ± 0.7	0.013 ± 0.002	72.82 ± 0.8
S7	225	NHT	5	125 ± 2.8	2.73 ± 0.3	112 ± 2.5	3.99 ± 0.4	51.79 ± 1.8	46.61 ± 1.9	758.8 ± 2.2	2.52 ± 0.6	0.026 ± 0.001	37.01 ± 1.0
S8	225	HT	3	98.5 ± 2.1	3.36 ± 0.3	88.7 ± 2.0	3.78 ± 0.3	40.97 ± 1.0	36.88 ± 1.0	487.7 ± 1.8	1.74 ± 0.3	0.025 ± 0.001	39.75 ± 1.0

ascertained. However, similar observations may be made by minimizing the strain values.

As observed in table 3, the processing condition comes out as the only significant parameter at a 95% confidence level. Also, it has been observed that the error % is well below 5% thus justifying the selection of the processing parameters. Based on table 3, figure 3 shows the best set of parameters for filament fabrication (210°C processing temperature, NHT as processing condition, and 5rpm extrusion speed). As observed in figure 3, the SN ratio for E decreased up to 220°C processing temperature, after that it has shown an increasing trend at 225°C. This may be because with a temperature rise say up to 220°C the flow property may have increased (in terms of MFI), but after that, the material may have more crystalline behavior because of the melt processing temperature. The processing condition as NHT and speed of 5 rpm may be because of the controlled heat input required for melt processing of R-PET used in this study.

The interaction effect for the observed properties has not been considered in this work, as here the main consideration is to reuse, R-PET for sensory applications. For further 3D printing, the feedstock filament was prepared at 210°C, processing conditions NHT and 5 rpm. As observed in table 2, for all processing temperatures, NHT as a processing condition resulted in better E. For example, while comparing samples S5 and S6, it has been ascertained that porosity% (as per ASTM B 276) was less in NHT sample S5 as compared to HT sample S6 (figure 4). The other surface characteristics based upon scanning electron microscopic (SEM) images for samples S5 and S6 are shown in figure 5, which justifies better surface properties for the NHT sample (S5) in terms of the 3D rendered image, amplitude distribution function (ADF), bearing ratio curve (BRC), peak count (PC) and surface roughness (Ra) (at a cut-off length of 0.05 mm) profile.

3.3 3D printing, ring resonator testing and HFSS analysis

A 1 mm thick rectangular strip of R-PET (size 30×40 mm²) was 3D printed on an FDM system keeping nozzle temperature 240°C, bed temperature 50°C, infill density 100%, and rectilinear printing fashion (figure 6). The printed prototypes were used to fabricate a designed ring resonator at the same settings (figure 7). The ring resonator dimensions are listed in table 4.

The fabricated 2-port ring resonator was tested on the VNA unit (figure 8) and observations were recorded for resonance of the prototype/resonator. Ports of ring resonator were connected (to port 1 and port 2) and values were measured for a span of 2 GHz (2 GHz to 4 GHz). It was observed that the functional prototype was resonating at 3.114 GHz and had an insertion loss of -26.27dB.

Table 3. Analysis of Variance for SN ratio (of E).

Source	Degree of freedom	A sequential sum of squares	Fisher's value	Probability (P%)	% Contribution
Processing temperature	3	2.7108	3.56	0.227	20.16
Processing condition	1	6.2252	24.54	0.038	46.29
Speed	1	3.9990	15.77	0.058	29.75
Residual Error	2	0.5073	–	–	3.77
Total	7	13.4423	–	–	–

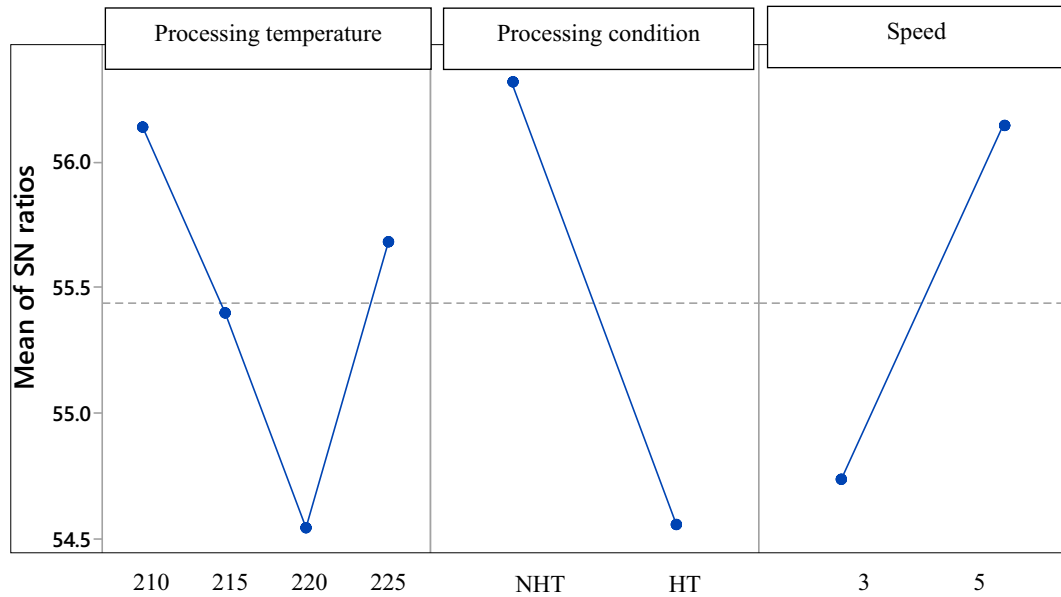


Figure 3. Main effect plot and ANOVA results for E of R-PET filament samples.

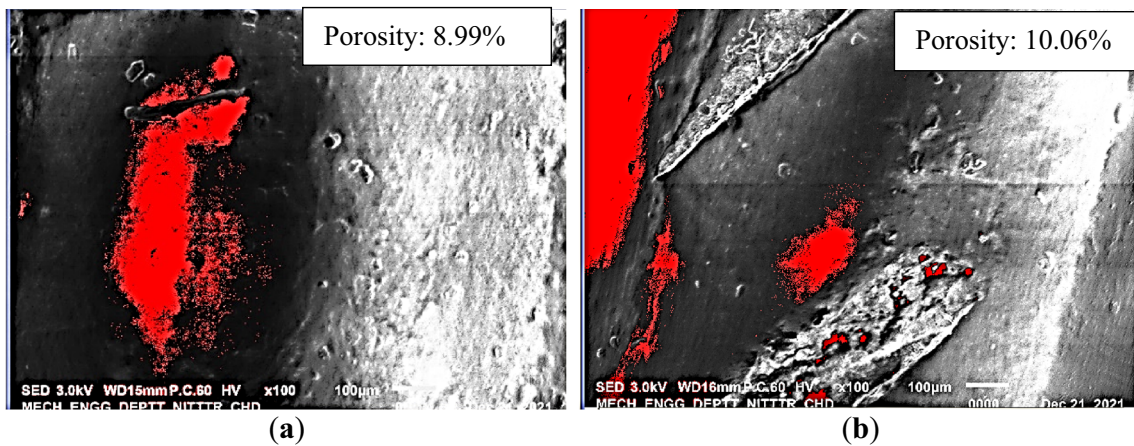


Figure 4. Porosity (%) of samples S5 (a), and S6 as per table 2 (b).

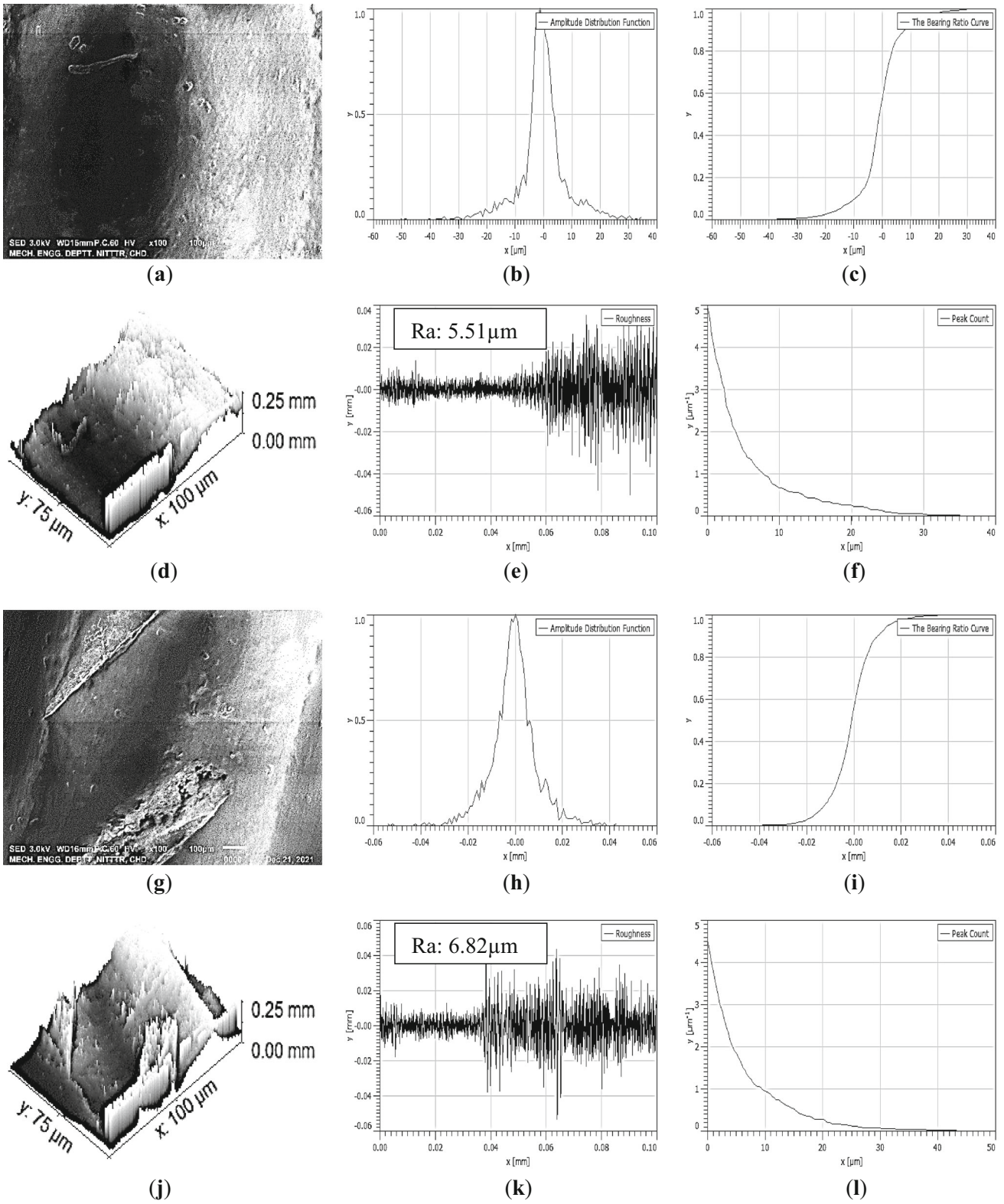


Figure 5. SEM image (a), ADF (b), BRC (c), 3D rendered image (d), Ra profile (e), PC (f) of sample S5 and SEM image (g), ADF (h), BRC (i), 3D rendered image (j), Ra profile (k), PC (l) of sample S6 as per table 2 (b).

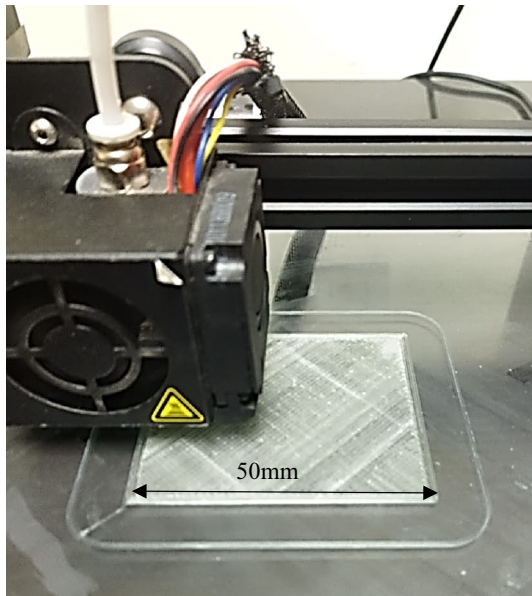


Figure 6. 3D printing of R-PET samples.

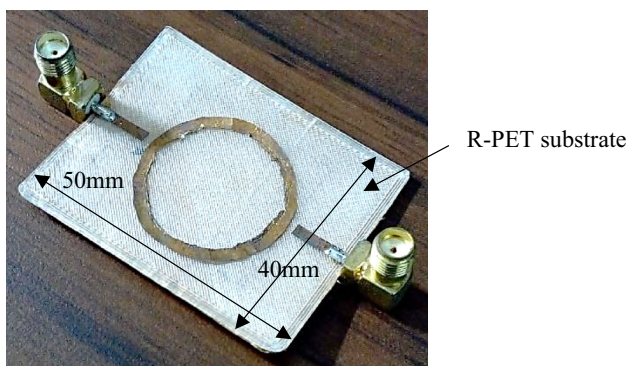


Figure 7. Ring resonator (used in the present study).

Table 4. Dimensions of 3D printed R-PET substrate-based ring resonator.

Parameters	Values
Mean radius	12.5 mm
Width of the feed line	1.9 mm
Feedline length	10.65 mm
Coupling gap	0.9 mm
The total length of the substrate	50 mm
Total width of the substrate	40 mm
The inner radius of the ring	11.55 mm
The outer radius of the ring	13.45 mm

From the obtained results of VNA, the ϵ_r and $\tan\delta$ of the R-PET were calculated by using standard equations reported in previous studies [27, 28]. The ϵ_r 1.71, and $\tan\delta$ 0.0041 were calculated for the R-PET substrate. It may be noted that the ϵ_r for virgin PET is 3.5 and the reported E is 9GPa [29]. In the present case of R-PET, the E has been significantly reduced, but the available value of E is sufficient for the required applications (like sailcloth, sailing spinnakers, and food-grade containers). The degradation in mechanical and dielectric properties may be because of repeated thermal cycles employed in R-PET. It may be noted that a lower ϵ_r leads to larger dimensions of antennas. Hence, in antenna design, it is necessary to perform miniaturization techniques and/or have a compromise between the ϵ_r , antenna sizes, radiation efficiency, and bandwidth. These values were used to determine the required dimensions of the patch antenna for sensing applications. The patch antenna of length 46.31 mm and a width of 52.57 mm was obtained (to investigate/simulate the R-PET-based antenna, which is a part of the sensor as a passive component). Simulations of the R-PET patch antenna were performed on HFSS for a resonance frequency of 2.45 GHz. Figure 9 shows the HFSS-based simulation of results of the R-PET antenna for wireless applications like Bluetooth, wireless fidelity (Wi-Fi), and fabrication of conformal devices in sailcloth/sailing spinnaker for online location tracking/monitoring of boats in ship parking zones. The schematic for sensing/detection is shown in figure 10. The spinnaker pole is proposed to be used for hoisting the spinnakers and R-PET as a substrate for an antenna. Since the simulated antenna resonates at 2.40 GHz (well in the industrial scientific and medical (ISM) band), it may be used successfully for the proposed location tracking (through Bluetooth application) by using a smartphone of the user, hence not requiring any special hardware/software of haphazardly parked boats in coastal regions, especially in low-income countries. It may be noted that in the present study weathering effect on mechanical and electrical properties has not been considered, and sensor capabilities have been explored for room temperature ($\approx 30^\circ\text{C}$).

3.4 XRD and FTIR analysis

The crystallization and amorphous behavior of the NHT and HT R-PET were tested by XRD analysis. A monochromatic X-ray beam of wavelength (λ) 0.154 nm generated from Cu-K- α transition was allowed to strike R-PET samples between the range of 5-95° angles. The hump observed in the samples for a 10-25° value of 2 θ confirmed the presence of a complete amorphous phase in R-PET. The XRD plot was observed for the HT R-PET

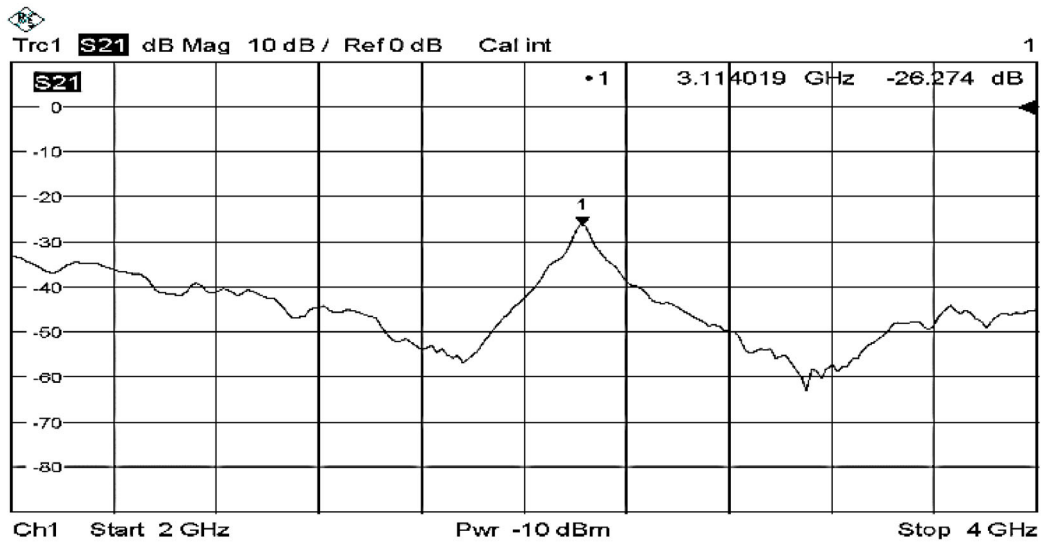


Figure 8. Resonance peak obtained for R-PET-based sensor/ring resonator.

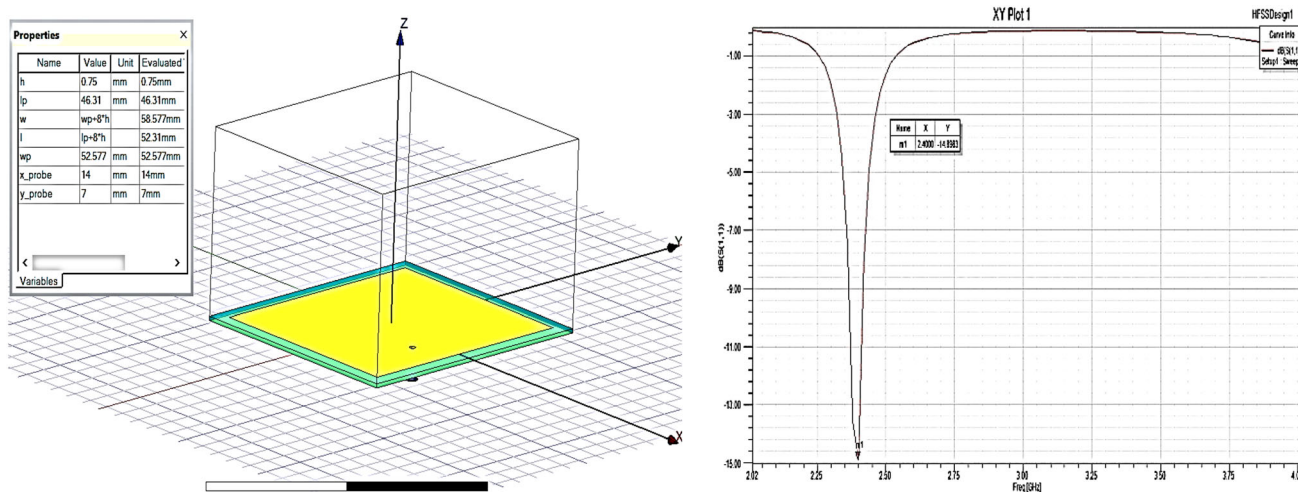


Figure 9. HFSS-based simulations for the resonance of R-PET substrate antenna.

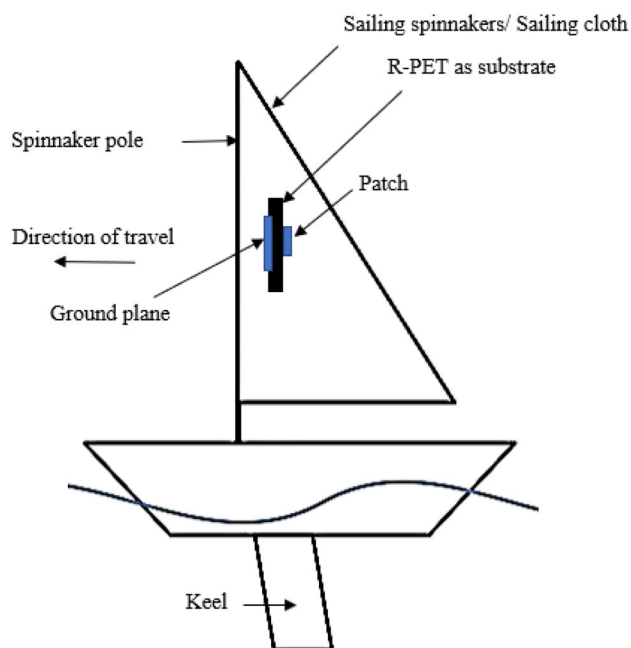


Figure 10. Schematic of sensing/detection.

sample and the NHT sample. The marginal shift in XRD peaks of the HT sample in figure 11a outlined that after HT, the increase in processing temperature resulted in the achievement of some crystallinity in PET leading to good rheological, and mechanical properties. These observations

are in line with tables 1 and 2, as it has been ascertained that after HT in general MFI and strain values got improved.

The absorbance peaks are shown in figure 11b and c for NHT and HT R-PET samples obtained from FTIR analysis. Infrared (IR) waves with wavelengths varying from 4500 to 500 cm^{-1} wave number (WN) were incident on extruded samples to obtain the absorbance spectrum. In the case of the NHT sample, asymmetrical stretching of the C-H bond was observed at 2850 cm^{-1} along with stretching of $-\text{C}(=\text{O})-\text{O}-$ group at 1250 cm^{-1} and bending of $-\text{CH}_2-$ group at 1735 cm^{-1} . In the case of the HT sample, the lower amplitude of absorbance peaks for $-\text{C}(=\text{O})-\text{O}-$ and $-\text{CH}_2-$ were noticed. But the peak at 2352 cm^{-1} for C-H stretching was high in the HT sample as compared to the same peak in the NHT sample. Therefore, FTIR analysis indicated that after the HT process, the formation of strong C-H bonds resulted in the formation of a crystalline lattice to improve the morphological and surface properties of R-PET.

It may be noted that the cost of virgin PET is ≈ 1.0 US \$/kg and recycled PET is $\approx 0.4-0.6$ US \$/kg. As regards the life cycle assessment of post-consumer R-PET, there have been reports about better environmental gains achieved from mechanical recycling when compared to landfill disposal or incineration, and the total energy required for R-PET bottles is 14-17% of the virgin PET manufacture [30, 31]. R-PET, when compared to virgin PET fibers, can save between 45 and 85% of non-renewable energy use, being connected with the reduction of global warming potential [31], therefore is recommended for the fabrication of value-added products.

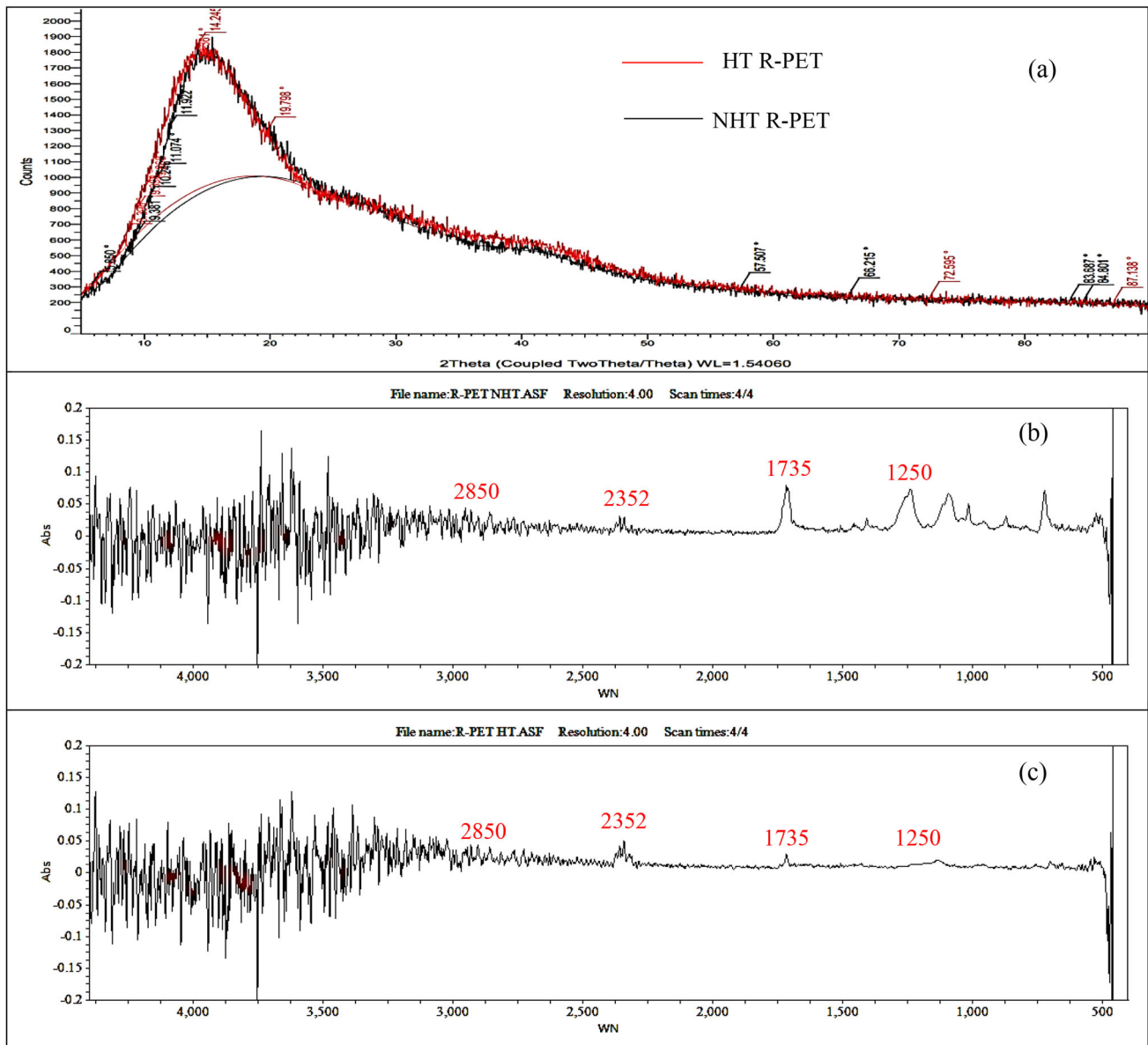


Figure 11. XRD (a), FTIR results for NHT, (b) HT and (c) R-PET.

4. Conclusions

The following are the conclusions from the present study:

- The recycling of PET for the preparation of 3D printed sensors (for location tracking/monitoring of boats) is possible through Bluetooth application (as PET is commercially being used as a sailcloth/sailing spinnaker). The PSW of R-PET may be shredded conveniently and extruded for the preparation of filament required for 3D printing.
- The rheological analysis based on the MFI test outlined that 230°C is the acceptable temperature to ascertain the flowability of R-PET. However, the best set of parameters for filament fabrication (of R-PET) is 210°C processing temperature, NHT as processing condition and 5 rpm extrusion speed.
- As regards V-I, XRD, and FTIR properties, the R-PET possesses acceptable electrical, and bonding capabilities for sensor applications. The VNA results and HFSS-based simulation support the outcomes of the

study, as the sensor may be used to sense the target within the Blue-tooth range of the ISM band.

Acknowledgements

The research has been partially funded under NTU-PU collaborated project and the Department of Science and Technology, (GoI) provided research facilities under the FIST project (File No. SR/FST/COLLEGE/2020/997).

Declaration

Conflict of interest The authors declare that no potential conflict of interest in the present study concerning the publication, research, and authorship.

References

- [1] Yang Z J, Harkin-Jones E M A, Armstrong C G and Menary G H 2004 Finite element modeling of stretch-blow molding of PET bottles using Buckley model: Plant tests and effects of process conditions and material parameters. *Proceedings of the Institution of Mechanical Engineers, Part E: Journal of Process Mechanical Engineering* 218: 237–250
- [2] Craggs G 1990 Mechanics analysis of the die drawing process for producing oriented polyethylene terephthalate (PET) tube. *Proceedings of the Institution of Mechanical Engineers, Part E: Journal of Process Mechanical Engineering* 204: 43–50
- [3] Małek M, Grzelak K, Łasica W, Jackowski M, Kluczyński J, Szachogluchowicz I, Torzewski J and Łuszczek J 2022 Cement-glass composite bricks (CGCB) with interior 3D printed PET-G scaffolding. *Journal of Building Engineering* 28: 104429
- [4] Aberoumand M, Soltanmohammadi K, Soleyman E, Rahmatabadi D, Ghasemi I, Baniassadi M, Abrinia K and Baghani M 2022 A comprehensive experimental investigation on 4D printing of PET-G under bending. *Journal of Materials Research and Technology* 18: 2552–2569
- [5] Laville S and Taylor M 2017 A million bottles a minute: world's plastic binge 'as dangerous as climate change. *The Guardian* 28: 2017
- [6] Boparai K S, Kumar A and Singh R 2022 Primary and secondary melt processing for plastics. In: *Book Additive Manufacturing for Plastic Recycling*, pp. 51–64. <https://doi.org/10.1201/9781003184164-4>
- [7] Kumar V, Singh R and Ahuja IPS, Tertiary recycling of plastic solid waste for additive manufacturing. In: *Book Additive Manufacturing for Plastic Recycling*, pp. 93–109. <https://doi.org/10.1201/9781003184164-6>
- [8] Jiang H, Jiang D, Liu X and Yang J 2021 A self-driven PET chip-based imprinted electrochemical sensor for the fast detection of Salmonella. *Sensors and Actuators B: Chemical* 349: 130785
- [9] Yang W, Weng C, Li X, Xu W, Fei J, Hong J, Zhang J, Zhu W and Zhou X 2022 An “on-off” ratio photoluminescence sensor based on catalytically induced PET effect by Fe₃O₄ NPs for the determination of coumarin. *Food Chemistry* 368: 130838
- [10] Zhao X, Yan Y, Wen J, Li Y and Li L 2022 Enhancement of magneto-caloric effect in all-d-metal Heusler Mn_{52.6}Ni_{30.5}-Co_{7.8}Ti_{9.1}/PVA/PET flexible composite by mechanical strains. *Journal of Alloys and Compounds* 897: 163116
- [11] Özen A, Ganzosch G, Barchiesi E, Auhl D W and Müller W H 2021 Investigation of deformation behavior of PETG-FDM-printed metamaterials with pantographic substructures based on different slicing strategies. *Composites and Advanced Materials* 30: 1–13
- [12] Schneevogt H, Stelzner K, Yilmaz B, Abali B E, Klunker A and Völlmecke C 2021 Sustainability in additive manufacturing: exploring the mechanical potential of recycled PET filaments. *Composites and Advanced Materials* 30: 1–8
- [13] Paesano A, Cohee D and Palmese G R 2003 Carbon-fiber reinforced thermoplastic materials for rigidizable space systems. *Journal of Thermoplastic Composite Materials* 16: 139–170
- [14] Tomaszewski G, Jankowski-Miśkiewicz P, Potencki J, Pietrikova A and Lukacs P 2022 Inkjet-printed HF antenna made on PET substrate. *Microelectronics Reliability* 129: 114473
- [15] Liu Q, Yi C, Chen J, Xia M, Lu Y, Wang Y, Liu X, Li M, Liu K and Wang D 2021 Flexible, breathable, and highly environmental-stable Ni/PPy/PET conductive fabrics for efficient electromagnetic interference shielding and wearable textile antennas. *Composites Part B: Engineering* 215: 108752
- [16] Kumar V, Singh R, Ahuja I P and Davim J P 2021 On nanographene-reinforced polyvinylidene fluoride composite matrix for 4D applications. *Journal of Materials Engineering and Performance* 30: 4860–4871
- [17] Zeng J J, Zhuge Y, Liang S D, Bai Y L, Liao J and Zhang L 2022 Durability assessment of PEN/PET FRP composites based on accelerated aging in alkaline solution/seawater with different temperatures. *Construction and Building Materials* 327: 126992
- [18] Kumar V, Singh R and Ahuja I P S 2022 On the programming of polyvinylidene fluoride–limestone composite for four-dimensional printing applications in heritage structures. *Proceedings of the Institution of Mechanical Engineers, Part L: Journal of Materials: Design and Applications* 236: 319–33
- [19] Griffin J C 1996 Evaluation of pet and recycled pet as replacements for a petg packaging tray. *Journal of Plastic Film & Sheeting* 12: 139–148
- [20] Gileno L A and Turci L F 2021 Life cycle assessment for PET-bottle recycling in Brazil: B2B and B2F routes. *Cleaner Environmental Systems* 3: 100057
- [21] Jiang Z, Yan D, Xin J, Li F, Guo M, Zhou Q, Xu J, Hu Y and Lu X 2022 Poly (ionic liquid) as efficient and recyclable catalysts for methanolysis of PET. *Polymer Degradation and Stability* 19: 109905
- [22] Kumar S, Singh R, Singh AP and Wei Y 2022 Case study for the development of a hybrid composite structure of thermosetting and thermoplastics. In: *Book Additive Manufacturing for Plastic Recycling* 141–157
- [23] Kumar R, Kumar V and Kumar P 2022 Secondary Recycling of HDPE Waste Thermoplastic by Mn Doped ZnO Nanoparticles Reinforcement. In: *Encyclopedia of Materials: Plastics and Polymers*, pp. 516–523

- [24] Kumar V, Singh R and Ahuja I P S 2022 Secondary recycled acrylonitrile–butadiene–styrene and graphene composite for 3D/4D applications: rheological, thermal, magnetometric, and mechanical analyses. *Journal of Thermoplastic Composite Materials* 35: 761–781
- [25] Kangavar M E, Lokuge W, Manalo A, Karunasena W and Frigione M 2022 Investigation on the properties of concrete with recycled polyethylene terephthalate (PET) granules as fine aggregate replacement. *Case Studies in Construction Materials* 16: e00934
- [26] Kumar V, Singh R and Ahuja I P S 2022 On rheological, thermal, mechanical, morphological, and piezoelectric properties and one-way programming features of polyvinylidene fluoride–CaCO₃ composites. *Journal of Materials Engineering and Performance* 1–15
- [27] Singh R, Kumar S, Singh A P and Wei Y 2022 On comparison of recycled LDPE and LDPE–bakelite composite based 3D printed patch antenna. *Proceedings of the Institution of Mechanical Engineers, Part L: Journal of Materials: Design and Applications* 236: 842–856
- [28] Jain C, Singh R and Dhaliwal B S 2022 On 3D printed ABS based sensors: rheological, mechanical, morphological, rf and 4d capabilities. *Journal of Materials Engineering and Performance* 1–15
- [29] Konieczna M, Markiewicz E and Jurga J 2010 Dielectric properties of polyethylene terephthalate/polyphenylene sulfide/barium titanate nanocomposite for application in electronic industry. *Polymer Engineering & Science* 50: 1613–1619
- [30] Gere D and Czigany T 2020 Future trends of plastic bottle recycling: compatibilization of PET and PLA. *Polymer Testing* 81: 106160
- [31] Sadeghi B, Marfavi Y, AliAkbari R, Kowsari E, Borbor Ajdari F and Ramakrishna S 2021 Recent studies on recycled PET fibers: production and applications: a review. *Materials Circular Economy* 3: 1–18